

Out-of-time-ordered-correlator quasiprobabilities robustly witness scrambling

José Raúl González Alonso,^{1,*} Nicole Yunger Halpern,² and Justin Dressel^{1,3}

¹*Schmid College of Science and Technology, Chapman University, Orange, CA 92866, USA*

²*Institute for Quantum Information and Matter, Caltech, Pasadena, CA 91125, USA*

³*Institute for Quantum Studies, Chapman University, Orange, CA 92866, USA*

(Dated: December 14, 2024)

Out-of-time-ordered correlators (OTOCs) have received considerable recent attention as qualitative witnesses of information scrambling in many-body quantum systems. Theoretical discussions of OTOCs typically focus on closed systems, raising the question of their suitability as scrambling witnesses in realistic open systems. We demonstrate that nonclassicality of the quasiprobability distribution (QPD) behind the OTOC is a more sensitive witness for scrambling than the OTOC itself. Nonclassical features of the QPD evolve with time scales that are robust with respect to decoherence and are immune to false positives caused by decoherence. To reach this conclusion, we numerically simulate spin-chain dynamics and three experimental protocols for measuring OTOCs: interferometric, quantum-clock, and weak-measurement. We target implementations with quantum-computing hardware such as superconducting qubits or trapped ions.

Introduction—Quantum many-body dynamics is *scrambling* when it causes initially localized quantum information to spread via entanglement through many degrees of freedom. Out-of-time-ordered correlators (OTOCs) have been suggested as a way to characterize scrambling [1–22]. As such, investigating how to measure OTOCs experimentally is crucial. Different OTOC-measurement protocols have been proposed [23–26], and some experimental success has been reported [27–30]. While OTOCs are being intensely investigated across condensed-matter and high-energy contexts [31–36], their robustness in realistic, decohering experimental settings has just started to be explored and is beginning to emerge as an active area of research [30, 37–41].

In this paper, we study decoherence’s effects on OTOCs being used to witness information scrambling. We find that their underlying quasiprobability distributions (QPDs) can more robustly identify the key time scales that distinguish scrambling. These QPDs are extended Kirkwood-Dirac QPDs [25, 42–47]. They reduce to classical joint probability distributions over the eigenvalues of the OTOC operators when the operators commute. However, for noncommuting operators, the QPDs become nonclassical: while the distribution remains normalized, individual quasiprobabilities can become negative, exceed one, or become nonreal. This nonclassicality robustly distinguishes scrambling from decoherence.

To illustrate decoherence’s effects on OTOCs, we must specify a measurement protocol. We study three: the (1) interferometric [24], (2) sequential-weak-measurement [25, 42], and (3) quantum-clock [26] protocols. Scrambling causes the OTOC to decay over a short time interval and then remain small. However, information leakage due to decoherence can reproduce this behavior [38], since a decohered system entangles with the environment. Thus, while quantum information spreads across many degrees of freedom, most of them are outside the system. We therefore propose a modification to these protocols

that uses the (coarse-grained) QPD behind the OTOC to distinguish between scrambling and nonscrambling dynamics despite decoherence. Additionally, we investigate the effects of dissipation on measurements of the (coarse-grained) QPD.

We find that decoherence can reproduce the qualitative decay of OTOCs usually associated with scrambling. As expected, OTOCs obtained with measurement protocols that require the longest laboratory time decay the most in the presence of decoherence. Additionally, we find that the QPD more reliably flags decoherence than the OTOC does. Moreover, the time scales associated with the loss of the QPD’s nonclassical behavior clearly distinguish dynamics with scrambling even in the presence of decoherence.

Our paper is organized as follows. We first define the OTOC and the QPD underlying it. As a concrete example suitable for simulation with qubit architectures, we consider a spin chain that can be toggled between scrambling and integrable dynamics. Next, we introduce dephasing, inspired by current superconducting-qubit technology, and analyze its effect on the OTOC and its QPD. We show numerical simulations of the spin chain for each OTOC-measurement protocol, and we compare their degradation due to decoherence. The numerical simulations also show that the QPD’s nonclassicality clearly distinguishes scrambling dynamics even when the OTOC behavior is ambiguous.

OTOCs and their quasiprobabilities—Quantum information scrambling is related to the quantum butterfly effect. Localized operators’ supports grow under time evolution by an appropriate Hamiltonian (e.g., a nonintegrable one). The initially local operators come to have large commutators with most other operators—even operators localized far from the initially considered and initially local operator. As an example, consider a Pauli operator acting locally on one end of a spin chain. We use another local Pauli operator defined on the opposite

side of the chain to probe the propagation of entanglement and quantum information. If the Hamiltonian is scrambling, an increasing number of degrees of freedom would need to be measured to recover the initially local information. Below, we make this intuition and its relation to the OTOC more precise.

Let H denote a quantum many-body system Hamiltonian; W and V local far-apart operators; and ρ a density matrix. The OTOC is defined as

$$F(t) := \text{Tr} (W^\dagger(t) V^\dagger W(t) V \rho). \quad (1)$$

Here, $W(t) = U(t)^\dagger W U(t)$ is evolved in the Heisenberg picture with the unitary evolution operator $U(t)$ generated by H . We assume that, initially, W and V commute: $[W(0), V] = 0$. If W and V are also unitary, then the OTOC is related to the Hermitian square of their commutator by

$$C(t) := \left\langle \frac{[W(t), V]^\dagger [W(t), V]}{(2i)^*} \frac{1}{2i} \right\rangle = \frac{1 - \text{Re } F(t)}{2}. \quad (2)$$

Otherwise, the commutator's square includes other terms involving nontrivial time-ordered correlators. A Hamiltonian that scrambles information tends to grow the commutator's magnitude. This growth leads to a persistent smallness of $\text{Re } F(t)$. In contrast, for a nonscrambling Hamiltonian, $W(t)$ and V approximately commute after a short amount of time, as information quickly recollects from other parts of the system. Therefore, $\text{Re } F(t)$ would exhibit revivals returning to close to one.

W and V decompose as $W = \sum_w w \Pi_w^W$ and $V = \sum_v v \Pi_v^V$, where Π_w^W and Π_v^V are the projectors onto the eigenspaces corresponding to the eigenvalues w and v . The eigenspaces are highly degenerate, since W and V are local operators and the system is large. $F(t)$ can be expressed as an average of eigenvalues [48],

$$F(t) = \sum_{v_1, w_2, v_2, w_3} v_1 w_2 v_2^* w_3^* \tilde{p}_t(v_1, w_2, v_2, w_3), \quad (3)$$

with respect to an extended Kirkwood-Dirac [43, 44] (*coarse-grained*) *quasiprobability distribution (QPD)*

$$\tilde{p}_t(v_1, w_2, v_2, w_3) := \text{Tr} \left(\Pi_{w_3}^{W(t)} \Pi_{v_2}^V \Pi_{w_2}^{W(t)} \Pi_{v_1}^V \rho \right). \quad (4)$$

\tilde{p}_t was denoted by $\tilde{\mathcal{A}}_\rho$ in [25].

Equation (3) implies that the QPD \tilde{p}_t exhibits the same time scales as the OTOC. Therefore, we should expect that qualitative features of OTOCs that reflect scrambling should have counterparts in \tilde{p}_t .

The QPD \tilde{p}_t is complex. However, like a classical probability distribution, it is normalized: $\sum_{v_1, w_2, v_2, w_3} \tilde{p}_t(v_1, w_2, v_2, w_3) = 1$. Therefore, regions where \tilde{p}_t becomes negative, exceeds one, or has a nonzero imaginary part are nonclassical. Hence, we introduce the

total nonclassicality of \tilde{p}_t as a measure of nonclassicality:

$$\tilde{N}(t) := \sum_{v_1, w_2, v_2, w_3} |\tilde{p}_t(v_1, w_2, v_2, w_3)| - 1. \quad (5)$$

As we will see in examples, even in the presence of decoherence, the total nonclassicality's evolution distinguishes integrable from nonintegrable Hamiltonians. The distinction allows the QPD to serve as a robust witness for scrambling.

Spin chain—We illustrate with a quantum Ising chain of N qubits. For ease of comparison, we use the conventions in [49–52]:

$$H = -J \sum_{i=1}^{N-1} \sigma_i^z \sigma_{i+1}^z - h \sum_{i=1}^N \sigma_i^z - g \sum_{i=1}^N \sigma_i^x. \quad (6)$$

We set $\hbar = 1$, such that energies are measured in units of J ; and times, in units of $1/J$. We fix $2\pi/J = 1 \mu s$ and simulate two cases:

1. Integrable case: $h/J = 0.0$, $g/J = 1.05$
2. Nonintegrable case: $h/J = 0.5$, $g/J = 1.05$.

We have chosen these values to match those of Ref. [25]. For the same reason, we have chosen $W = \sigma_1^z$ and $V = \sigma_N^z$ [53].

To map this Hamiltonian onto a physical qubit system, e.g., an array of transmons [54, 55], we interpret the eigenstates of $-\sigma_i^x$ as the energy eigenbasis of each qubit. Each qubit has an intrinsic energy splitting of $2g$ and is capacitively coupled to its neighbors with energy J . Each qubit is driven at a Rabi frequency $2h$, and the drive can be turned on and off. Unless prepared by a measurement, such a qubit system relaxes to a thermal state as a natural preparation. Therefore, as an initial state, we consider a Gibbs state at finite temperature T : $\rho_T = \mathcal{Z}^{-1} \exp(-H/T)$ with $T/J = 1$, $\mathcal{Z} = \text{Tr}(\exp(-H/T))$, and $k_B = 1$ [56]. Each qubit has a ground-state population of approximately 0.2. OTOCs are usually evaluated on thermal states due to holographic interest in the thermofield double state [3, 4, 6–10, 12, 13, 17].

Decoherence—To numerically model decoherence, we use a Lindblad master equation $d\rho/dt = -i[H, \rho] + \sum_{i=1}^{N+n_a} \gamma_i \left(L_i \rho L_i^\dagger - 1/2 \{L_i^\dagger L_i, \rho\} \right)$. Here, N denotes the number of spins in the chain; and n_a , the number of ancillas required for a given protocol. We choose $L_i = \sigma_i^z$ and $\gamma_i = \gamma = 1/(2T_2^*)$. The operators L_i implement single-qubit dephasing at rates γ_i since environmental dephasing is the dominant limitation of system coherence prior to relaxation. The parameter T_2^* denotes the observed exponential decay constant for the qubit coherence from chip-dependent environmental fluctuations. We have chosen an optimistic $T_2^* = 130 \mu s$, which is plausible for upcoming transmon hardware [57]. We interpret

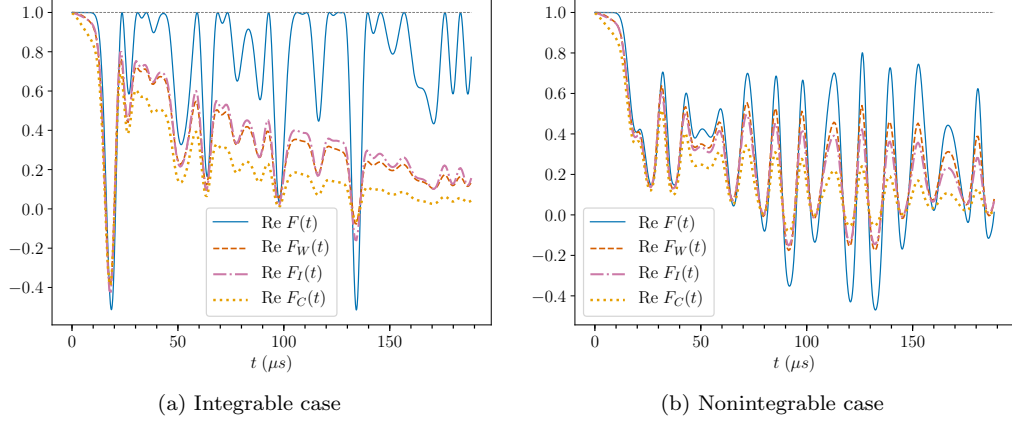


Figure 1. Evolution of measured OTOC, $F(t) = \langle W^\dagger(t)V^\dagger W(t)V \rangle$, with and without decoherence. Values measured with three different protocols are compared against the ideal value: interferometric $F_I(t)$, weak $F_W(t)$, and quantum clock $F_C(t)$. The system consists of $N = 5$ spins in an Ising chain with (a) a transverse field and (b) a transverse and a longitudinal field, with parameters detailed in the text. The system starts in a Gibbs state $\rho_T = \mathcal{Z}^{-1} \exp(-H/T)$ with $T/J = 1$ and $\mathcal{Z} = \text{Tr}(\exp(-H/T))$. The system undergoes environmental dephasing of each qubit with a decay constant of $T_2^* = 130 \mu\text{s}$. The local operators $W = \sigma_1^z$ and $V = \sigma_N^z$. These plots highlight the difficulties in unambiguously distinguishing between (a) nonscrambling and (b) scrambling Hamiltonians in an experimental setting with decoherence.

the Lindblad equation as an average over the stochastic phase-jumps that could occur during each time step dt . Such a jump updates a density matrix ρ according to

$$\rho \mapsto dt \sum_i \gamma_i L_i U(t) \rho U(t)^\dagger L_i^\dagger + L_0 U(t) \rho U(t)^\dagger L_0^\dagger. \quad (7)$$

The no-phase-jump operator is $L_0 = \sqrt{\mathbb{1} - dt \sum_i \gamma_i L_i^\dagger L_i}$. We choose this numerical procedure because of its simplicity and numerical stability [58].

For all three OTOC-measurement protocols, we replace the usual time evolution by Eq. (7) and assume that, under decoherence, only the sign of the time evolution's unitary part, $U(t)$, is affected when a time reversal is called for. This is equivalent to reversing only the sign of H in the Lindblad equation's first term. We also distinguish between the total time elapsed in the laboratory, t_L , and the time t at which the OTOC is evaluated. Each simulated reversal of t accumulates positive lab time t_L ; thus, every protocol's t_L depends on t differently. To simulate decoherence's effects on the QPD, we use the weak-measurement protocol [25, 42]. Changes to the other protocols to make them adequate for QPD-measurements are also possible [25].

Simulation results and discussion—Figure 1 shows the real part of the OTOC, measured in the presence of decoherence: $F_I(t)$, $F_W(t)$, and $F_C(t)$ denote the OTOC measured according to the interferometric [24], weak-measurement [25, 42], and quantum-clock [26] protocols, respectively. These curves are compared to the ideal OTOC $F(t)$ measured in the absence of noise. These protocols differ in the amounts of lab time required to measure $F(t)$: the protocols need t_L 's that are at least

$2t$, $3t$, and $4t$, respectively. As expected, OTOCs measured with long- t_L protocols decay the most, since they suffer from decoherence the longest. The quantum-clock protocol's $F_C(t)$ is affected the most. Nonetheless, this protocol's essence—the implementation of time reversals via an ancilla qubit—could be combined with a shorter- t_L protocol (e.g., the interferometric protocol), to mitigate decoherence [59].

Figures 1a and 1b show that decoherence hinders us from easily distinguishing between integrable and nonintegrable Hamiltonians. The integrable-Hamiltonian OTOC with decoherence exhibits decay caused by information leaking, whereas the nonintegrable-Hamiltonian OTOC exhibits revivals. If we used these two OTOCs' qualitative behaviors, we would misclassify the Hamiltonians and incur a false positive, inferring scrambling where there is none.

Distinguishing scrambling from integrable Hamiltonians via the QPD is straightforward, even in the presence of decoherence (Fig. 2). Decoherence damps the distribution's oscillations, and the different curves drift towards a common value (in our example, between 0 and 0.1). On the other hand, unlike in the integrable case, the nonintegrable case's quasiprobability shows persistent pitchforks. These pitchforks arise because scrambling breaks a symmetry: scrambling eliminates the QPD's invariance under certain permutations and negations of the QPD arguments in Eq. (4) [25]. The symmetry breaking eliminates the QPD's constancy under certain interchanges, and certain flips, of measurement outcomes in the weak-measurement scheme. We should expect this asymmetry to be reflected in the total nonclassicality \tilde{N}_t

of Eq. (5). Since information scrambling is related to coherent many-body entanglement of the system, which is nonclassical, we expect the QPD’s nonclassicality to be a robust indicator of scrambling. Indeed, the negative regions in Fig. 2 are sensitively affected by the damping: as time progresses, they shrink. The negative regions also show structure that mirrors qualitative behavior of the OTOC: the decay of $\text{Re } F(t)$ matches the flourishing of the negativity; the revivals of $\text{Re } F(t)$ mirror the negativity’s disappearance.

We plot $\tilde{N}(t)$ in Fig. 3. The nonclassicality’s persistence reflects sustained noncommutativity of $W(t)$ and V . Several points merit attention. First, denote by \tilde{t}_* the point at which $\tilde{N}(t)$ first starts to deviate from zero [60]; by t_m , the point at which the first maximum occurs; and by t_z , the time at which the first zero after the first maximum happens. For the scrambling dynamics with decoherence in Fig. 3, $t_z - t_m$ is more than an order of magnitude longer than $t_m - \tilde{t}_*$. For the nonscrambling dynamics, the two time scales are comparable. Without dissipation, $t_z - t_m$ is even longer than the simulation time. We thus conjecture that, if $t_m - \tilde{t}_* \ll t_z - t_m$, the dynamics is scrambling. As the quantum information spreads throughout the system in a time $t_m - \tilde{t}_* \propto N$, if the system Hamiltonian H is integrable, the information recollects in a time $t_z - t_m \propto N$. Hence, the total nonclassicality’s first peak should be fairly symmetrical. If the system dynamics is scrambling, such a recollection would occur after a much longer time [17, 61, 62]. Therefore, $\tilde{N}(t)$ should display strong temporal asymmetry about its first maximum. We see this lack of symmetry in the scrambling case’s $\tilde{N}(t)$ in Fig. 3b. We also see the role of our conjecture in the presence of decoherence: because of the significant differences in the scrambling-case time scales, the asymmetry persists despite the dissipation’s suppression of $\tilde{N}(t)$. In contrast, $F(t)$ does not offer such a quantitative insight: $\tilde{N}(t)$ is useful because it precisely identifies the times at which nonclassical behavior arises or disappears.

Conclusions and outlook—We have seen that decoherence can cause the qualitative OTOC decay usually associated with scrambling. We observe that OTOCs measured with protocols that require long lab times t_L will decay the most. The quantum-clock protocol is the most affected but can be combined with the interferometric or weak-measurement protocols for better performance [59]. Additionally, two opportunities for improving the robustness and convenience of the QPD-measurement scheme in [25] exist. First, the weak measurements might be replaced with strong measurements, along the lines in [59]. Second, the renormalization scheme in [39] might be applied to mitigate errors.

We propose that a more robust witness can be found in the nonclassical part of the QPD \tilde{p}_t behind the OTOC. The total nonclassicality \tilde{N} of \tilde{p}_t helps distinguish integrable from scrambling Hamiltonians in the presence of

decoherence. One can distinguish clearly between scrambling and nonscrambling systems by comparing two time scales of \tilde{N} . The duration between the birth of nonclassicality, at the time \tilde{t}_* , and the nonclassicality’s first local maximum, at t_m , is related to the time needed by quantum information to spread throughout the system. The spreading’s persistence governs the duration between t_m and the death of nonclassicality, at t_z . Nonscrambling dynamics exhibits revivals of classicality on time scales $t_m - \tilde{t}_* \approx t_z - t_m$, while scrambling dynamics takes much longer. This distinction is clearly seen in the total nonclassicality $\tilde{N}(t)$. Unlike the OTOC, $\tilde{N}(t)$ is robust with respect to experimental imperfections like decoherence. Characterizing this time’s scaling with system size, and checking whether the scaling can be consistent with doubly exponential expectations inspired by the Poincaré recurrence time [17, 61, 62], is a subject for future research.

Another opportunity for future study is whether scrambling breaks symmetries in OTOC QPDs defined in terms of W and V operators other than qubit Pauli operators. An interesting choice to study next would be the Sachdev-Ye-Kitaev (SYK) model [7, 63]. The SYK model consists of Majorana fermions, whose experimental realizations are being pursued assiduously [64–70]. As the SYK model scrambles maximally quickly, like black holes, it has been hoped to shed light on quantum gravity. The calculational tools available for SYK merit application to the OTOC QPD, which may shed new light on scrambling at the intersection of condensed matter and high-energy physics.

Note added—During the final stages of this manuscript’s preparation, [40] was released. The authors propose another tack to separating scrambling from decoherence and focus on scrambling measures alternative to OTOCs [30, 33]. Our paper identifies the OTOC quasiprobability as a distinguisher and as a reliable scrambling signature in the context of OTOCs.

Acknowledgements—JRGA was supported by a fellowship from the Grand Challenges Initiative at Chapman University. NYH is grateful for funding from the Institute for Quantum Information and Matter, an NSF Physics Frontiers Center (NSF Grant PHY-1125565) with support from the Gordon and Betty Moore Foundation (GBMF-2644); a Graduate Fellowship from the Kavli Institute for Theoretical Physics, supported by the NSF under Grant No. NSF PHY-1125915; the Walter Burke Institute for Theoretical Physics at Caltech; and a Barbara Groce Graduate Fellowship. JD was partially supported by the Army Research Office (ARO) grant No. W911NF-15-1-0496. The authors wish to thank Paul Dieterle, Poul Jessen, Andrew Keller, Oskar Painter, and Mordecai Waegell for helpful discussions.

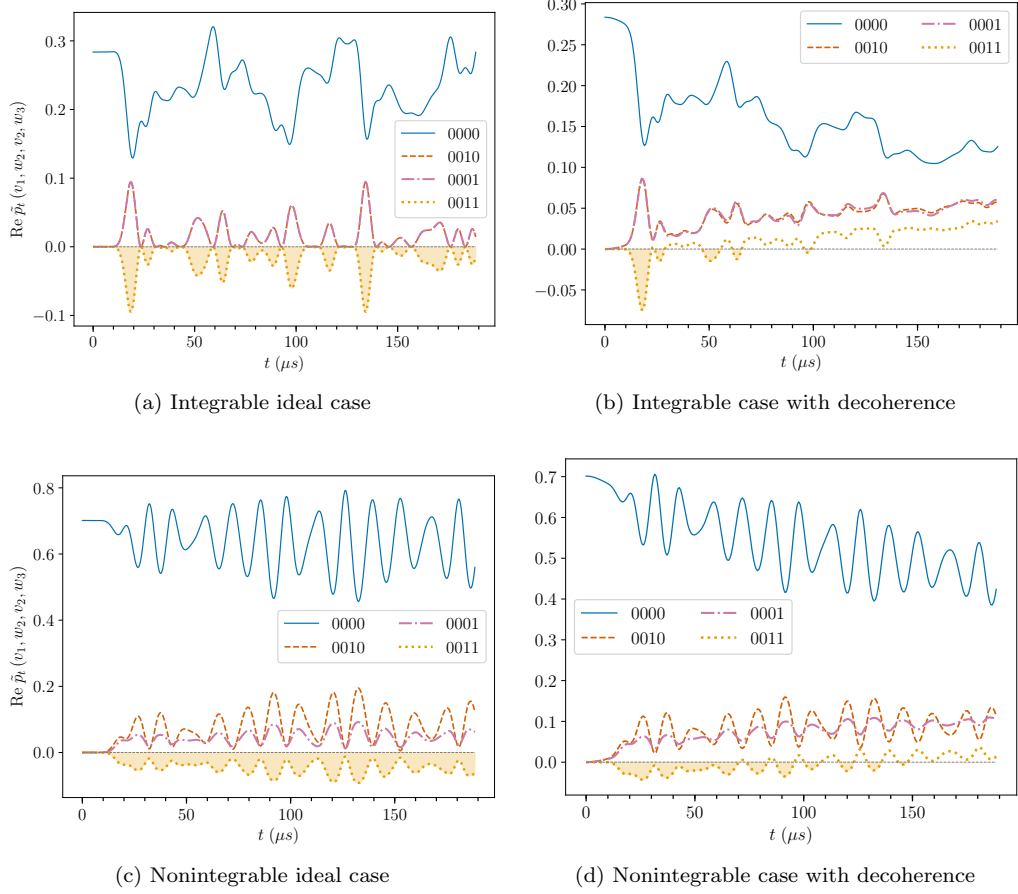


Figure 2. Evolution of measured $\text{Re } \tilde{p}_t$ with and without decoherence, using the sequential-weak-measurement protocol. The QPD, $\tilde{p}_t(v_1, w_2, v_2, w_3) = \text{Tr}(\Pi_{w_3}^{W(t)} \Pi_{v_2}^V \Pi_{w_2}^{W(t)} \Pi_{v_1}^V \rho)$, underlies the OTOC, $F(t) = \sum v_1 w_2 v_2^* w_3^* \tilde{p}_t(v_1, w_2, v_2, w_3)$, where $V = \sum v \Pi_v$ and $W = \sum w \Pi_w$. Of 16 QPD values, four examples are shown. The numeric labels in the legend have the form $abcd$, where $v_1 = (-1)^a$, $w_2 = (-1)^b$, $v_2 = (-1)^c$, and $w_3 = (-1)^d$. The shaded regions show nonclassical behavior of the QPD.

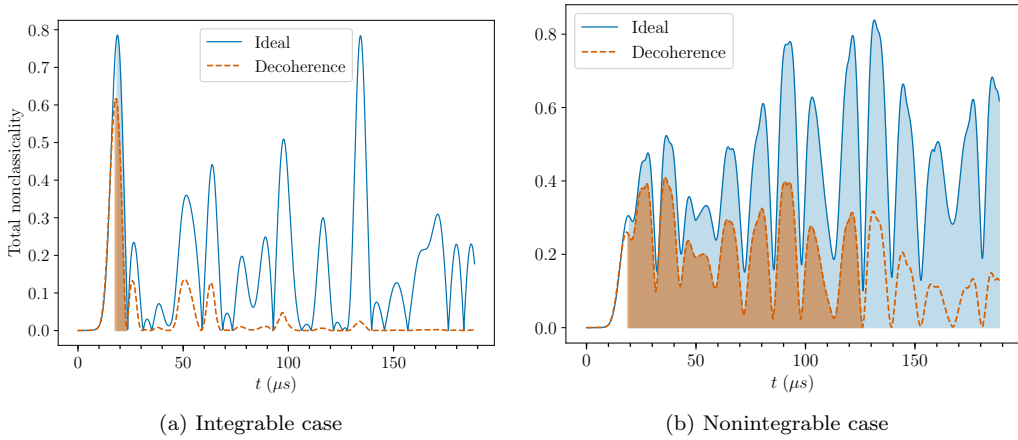


Figure 3. Total nonclassicality, $\tilde{N}(t) = \sum |\tilde{p}_t(v_1, w_2, v_2, w_3)| - 1$, of the QPD, \tilde{p}_t , showing sensitivity to decoherence for (a) integrable and (b) scrambling systems. Comparing two time scales can reveal scrambling. The duration between the onset of nonclassicality ($\tilde{t}_* \sim 10 \mu s$) and the first maximum ($t_m \sim 20 \mu s$) is roughly constant across all plots. The area between t_m and the next zero (t_z) is shaded. Without scrambling, $t_z - t_m \sim t_m - \tilde{t}_* \sim 10 \mu s$. With scrambling, $t_z - t_m$ remains an order of magnitude larger ($t_z - t_m \sim 100 \mu s$), even with decoherence. In the decoherence-free scrambling case, $\tilde{N}(t)$ remains large for at least four orders of magnitude of time longer than in the nonscrambling case.

-
- * Corresponding author: gonzalezalonso@chapman.edu
- [1] A. I. Larkin and Y. N. Ovchinnikov, “Quasiclassical Method in the Theory of Superconductivity,” *Soviet Journal of Experimental and Theoretical Physics* **28**, 1200 (1969).
 - [2] A. Kitaev, “Hidden correlations in the Hawking radiation and thermal noise, talk given at Fundamental Physics Prize Symposium,” (2014).
 - [3] S. H. Shenker and D. Stanford, “Black holes and the butterfly effect,” *Journal of High Energy Physics* **2014** (2014).
 - [4] S. H. Shenker and D. Stanford, “Multiple shocks,” *Journal of High Energy Physics* **12**, 46 (2014), [arXiv:1312.3296](#).
 - [5] S. A. Hartnoll, “Theory of universal incoherent metallic transport,” *Nature Physics* **11**, 54 (2015), [arXiv:1405.3651](#).
 - [6] S. H. Shenker and D. Stanford, “Stringy effects in scrambling,” *Journal of High Energy Physics* **5**, 132 (2015), [arXiv:1412.6087](#).
 - [7] A. Kitaev, “A Simple Model of Quantum Holography, KITP strings seminar and Entanglement,” (2015).
 - [8] D. A. Roberts, D. Stanford, and L. Susskind, “Localized shocks,” *Journal of High Energy Physics* **2015** (2015).
 - [9] D. A. Roberts and D. Stanford, “Diagnosing Chaos Using Four-Point Functions in Two-Dimensional Conformal Field Theory,” *Physical Review Letters* **115**, 131603 (2015), [arXiv:1412.5123](#).
 - [10] J. Maldacena, S. H. Shenker, and D. Stanford, “A bound on chaos,” *Journal of High Energy Physics* **8**, 106 (2016), [arXiv:1503.01409](#).
 - [11] I. L. Aleiner, L. Faoro, and L. B. Ioffe, “Microscopic model of quantum butterfly effect: Out-of-time-order correlators and traveling combustion waves,” *Annals of Physics* **375**, 378 (2016), [arXiv:1609.01251](#).
 - [12] M. Blake, “Universal Charge Diffusion and the Butterfly Effect in Holographic Theories,” *Physical Review Letters* **117**, 091601 (2016).
 - [13] M. Blake, “Universal diffusion in incoherent black holes,” *Physical Review D* **94**, 086014 (2016).
 - [14] Y. Chen, “Universal Logarithmic Scrambling in Many Body Localization,” *ArXiv e-prints* (2016), [arXiv:1608.02765](#).
 - [15] A. Lucas and J. Steinberg, “Charge diffusion and the butterfly effect in striped holographic matter,” *Journal of High Energy Physics* **2016**, 143 (2016).
 - [16] D. A. Roberts and B. Swingle, “Lieb-Robinson Bound and the Butterfly Effect in Quantum Field Theories,” *Physical Review Letters* **117**, 091602 (2016).
 - [17] P. Hosur, X.-L. Qi, D. A. Roberts, and B. Yoshida, “Chaos in quantum channels,” *Journal of High Energy Physics* **2**, 4 (2016), [arXiv:1511.04021](#).
 - [18] S. Banerjee and E. Altman, “Solvable model for a dynamical quantum phase transition from fast to slow scrambling,” *Physical Review B* **95** (2017), [arXiv:1610.04619](#).
 - [19] R. Fan, P. Zhang, H. Shen, and H. Zhai, “Out-of-time-order correlation for many-body localization,” *Science Bulletin* **62**, 707 (2017).
 - [20] Y. Gu, X.-L. Qi, and D. Stanford, “Local criticality, diffusion and chaos in generalized Sachdev-Ye-Kitaev models,” *Journal of High Energy Physics* **2017**, 125 (2017).
 - [21] D. A. Roberts and B. Yoshida, “Chaos and complexity by design,” *Journal of High Energy Physics* **4**, 121 (2017), [arXiv:1610.04903](#).
 - [22] X. Chen and T. Zhou, “Operator scrambling and quantum chaos,” *ArXiv e-prints* (2018), [arXiv:1804.08655](#).
 - [23] N. Y. Yao, F. Grusdt, B. Swingle, M. D. Lukin, D. M. Stamper-Kurn, J. E. Moore, and E. A. Demler, “Interferometric Approach to Probing Fast Scrambling,” *ArXiv e-prints* (2016), [arXiv:1607.01801](#).
 - [24] B. Swingle, G. Bentsen, M. Schleier-Smith, and P. Hayden, “Measuring the scrambling of quantum information,” *Physical Review A* **94**, 040302 (2016), [arXiv:1602.06271](#).
 - [25] N. Yunger Halpern, B. Swingle, and J. Dressel, “Quasiprobability Behind the Out-of-Time-Ordered Correlator,” *Physical Review A* **97**, 042105 (2018).
 - [26] G. Zhu, M. Hafezi, and T. Grover, “Measurement of many-body chaos using a quantum clock,” *Physical Review A* **94**, 062329 (2016), [arXiv:1607.00079](#).
 - [27] K. X. Wei, C. Ramanathan, and P. Cappellaro, “Exploring Localization in Nuclear Spin Chains,” *ArXiv e-prints* (2016), [arXiv:1612.05249](#).
 - [28] M. Gärttner, J. G. Bohnet, A. Safavi-Naini, M. L. Wall, J. J. Bollinger, and A. M. Rey, “Measuring out-of-time-order correlations and multiple quantum spectra in a trapped-ion quantum magnet,” *Nature Physics* **13**, 781 (2017), [arXiv:1608.08938](#).
 - [29] J. Li, R. Fan, H. Wang, B. Ye, B. Zeng, H. Zhai, X. Peng, and J. Du, “Measuring Out-of-Time-Order Correlators on a Nuclear Magnetic Resonance Quantum Simulator,” *Physical Review X* **7** (2017).
 - [30] K. A. Landsman, C. Figgatt, T. Schuster, N. M. Linke, B. Yoshida, N. Y. Yao, and C. Monroe, “Verified Quantum Information Scrambling,” *ArXiv e-prints* (2018), [arXiv:1806.02807](#).
 - [31] Y. Huang, Y.-L. Zhang, and X. Chen, “Out-of-time-ordered correlators in many-body localized systems,” *Annalen der Physik* **529**, 1600318 (2017), [arXiv:1608.01091](#).
 - [32] E. Iyoda and T. Sagawa, “Scrambling of Quantum Information in Quantum Many-Body Systems,” *ArXiv e-prints* (2017), [arXiv:1704.04850](#).
 - [33] B. Yoshida and A. Kitaev, “Efficient decoding for the Hayden-Preskill protocol,” *ArXiv e-prints* (2017), [arXiv:1710.03363](#).
 - [34] C.-J. Lin and O. I. Motrunich, “Out-of-time-ordered correlators in a quantum Ising chain,” *Physical Review B* **97**, 144304 (2018).
 - [35] S. Pappalardi, A. Russomanno, B. Žunkovič, F. Iemini, A. Silva, and R. Fazio, “Scrambling and entanglement spreading in long-range spin chains,” *ArXiv e-prints* (2018), [arXiv:1806.00022](#).
 - [36] N. Yunger Halpern, A. Bartolotta, and J. Pollack, “Reconciling two notions of quantum operator disagreement: Entropic uncertainty relations and information scrambling, united through quasiprobabilities,” *ArXiv e-prints* (2018), [arXiv:1806.04147](#).
 - [37] S. V. Syzranov, A. V. Gorshkov, and V. Galitski, “Out-of-time-order correlators in finite open systems,” *ArXiv e-prints* (2017), [arXiv:1704.08442](#).
 - [38] Y.-L. Zhang, Y. Huang, and X. Chen, “Information scrambling in chaotic systems with dissipation,” *ArXiv e-prints* (2018), [arXiv:1802.04492](#).
 - [39] B. Swingle and N. Yunger Halpern, “Resilience of scrambling measurements,” *Physical Review A* **97**, 062113 (2018).

- (2018).
- [40] B. Yoshida and N. Y. Yao, “Disentangling Scrambling and Decoherence via Quantum Teleportation,” *ArXiv e-prints* (2018), [arXiv:1803.10772](#).
 - [41] M. Knap, “Entanglement production and information scrambling in a noisy spin system,” *ArXiv e-prints* (2018), [arXiv:1806.04686](#).
 - [42] N. Yunger Halpern, “Jarzynski-like equality for the out-of-time-ordered correlator,” *Physical Review A* **95**, 012120 (2017), [arXiv:1609.00015](#).
 - [43] J. G. Kirkwood, “Quantum Statistics of Almost Classical Assemblies,” *Physical Review* **44**, 31 (1933).
 - [44] P. A. M. Dirac, “On the Analogy Between Classical and Quantum Mechanics,” *Reviews of Modern Physics* **17**, 195 (1945).
 - [45] Y. P. Terletsky, “The limiting transition from quantum to classical mechanics,” *Journ. Exper. Theor. Phys* **7**, 1290 (1937).
 - [46] H. Margenau and R. N. Hill, “Correlation between Measurements in Quantum Theory,” *Progress of Theoretical Physics* **26**, 722 (1961).
 - [47] S. Chaturvedi, E. Ercolessi, G. Marmo, G. Morandi, N. Mukunda, and R. Simon, “Wigner–Weyl correspondence in quantum mechanics for continuous and discrete systems—a Dirac-inspired view,” *Journal of Physics A: Mathematical and General* **39**, 1405 (2006).
 - [48] We index the W and V eigenvalues in Eq. (3) following the conventions in [25, 42].
 - [49] G. P. Berman, F. Borgonovi, F. M. Izrailev, and V. I. Tsifrinovich, “Delocalization border and onset of chaos in a model of quantum computation,” *Physical Review E* **64**, 056226 (2001), [quant-ph/0104086](#).
 - [50] M. C. Bañuls, J. I. Cirac, and M. B. Hastings, “Strong and Weak Thermalization of Infinite Nonintegrable Quantum Systems,” *Physical Review Letters* **106**, 050405 (2011).
 - [51] A. Gubin and L. F. Santos, “Quantum chaos: An introduction via chains of interacting spins $1/2$,” *American Journal of Physics* **80**, 246 (2012), [arXiv:1106.5557](#).
 - [52] H. Kim and D. A. Huse, “Ballistic Spreading of Entanglement in a Diffusive Nonintegrable System,” *Physical Review Letters* **111**, 127205 (2013).
 - [53] It is worth noting that, σ_x with an integrable Hamiltonian, can simulate scrambling. For details, see Ref. [34].
 - [54] R. Barends, J. Kelly, A. Megrant, D. Sank, E. Jeffrey, Y. Chen, Y. Yin, B. Chiaro, J. Mutus, C. Neill, P. O’Malley, P. Roushan, J. Wenner, T. C. White, A. N. Cleland, and J. M. Martinis, “Coherent Josephson Qubit Suitable for Scalable Quantum Integrated Circuits,” *Physical Review Letters* **111**, 080502 (2013).
 - [55] J. Koch, T. M. Yu, J. Gambetta, A. A. Houck, D. I. Schuster, J. Majer, A. Blais, M. H. Devoret, S. M. Girvin, and R. J. Schoelkopf, “Charge-insensitive qubit design derived from the Cooper pair box,” *Physical Review A* **76**, 042319 (2007).
 - [56] Additionally, this allows us to circumvent the difficulties associated with experimentally preparing an infinite-temperature Gibbs state.
 - [57] Private communication with Irfan Siddiqi.
 - [58] M. Khezri, J. Dressel, and A. N. Korotkov, “Qubit measurement error from coupling with a detuned neighbor in circuit QED,” *Physical Review A* **92** (2015).
 - [59] J. Dressel, J. R. González Alonso, M. Waegell, and N. Yunger Halpern, “Strengthening weak measurement of qubit out-of-time-order correlators,” *ArXiv e-prints* (2018), [arXiv:1805.00667](#).
 - [60] By virtue of this definition, \tilde{t}_* is close to the scrambling time t_* at which $\text{Re } F(t)$ first deviates significantly from one.
 - [61] P. Bocchieri and A. Loinger, “Quantum Recurrence Theorem,” *Physical Review* **107**, 337 (1957).
 - [62] L. Campos Venuti, “The recurrence time in quantum mechanics,” *ArXiv e-prints* (2015), [arXiv:1509.04352](#).
 - [63] S. Sachdev and J. Ye, “Gapless spin-fluid ground state in a random quantum Heisenberg magnet,” *Physical Review Letters* **70**, 3339 (1993).
 - [64] F. Hassler, “Majorana Qubits,” (2014), in “Quantum Information Processing. Lecture Notes of the 44th IFF Spring School 2013”, edited by D. P. DiVincenzo (Verlag des Forschungszentrums Jülich, 2013), [arXiv:1404.0897](#).
 - [65] D. Aasen, M. Hell, R. V. Mishmash, A. Higginbotham, J. Danon, M. Leijnse, T. S. Jespersen, J. A. Folk, C. M. Marcus, K. Flensberg, and J. Alicea, “Milestones toward Majorana-based quantum computing,” *Physical Review X* **6**, 031016 (2015).
 - [66] M. T. Deng, S. Vaitiekėnas, E. Prada, P. San-Jose, J. Nygård, P. Krogstrup, R. Aguado, and C. M. Marcus, “Majorana non-locality in hybrid nanowires,” *ArXiv e-prints* (2017).
 - [67] S. Vaitiekėnas, M. T. Deng, J. Nygård, P. Krogstrup, and C. M. Marcus, “Effective g-factor in Majorana Wires,” *ArXiv e-prints* (2017).
 - [68] R. M. Lutchyn, E. P. a. M. Bakkers, L. P. Kouwenhoven, P. Krogstrup, C. M. Marcus, and Y. Oreg, “Realizing Majorana zero modes in superconductor-semiconductor heterostructures,” *Nature Reviews Materials* **3**, 52 (2017).
 - [69] F. J. Gomez-Ruiz, J. J. Mendoza-Arenas, F. J. Rodriguez, C. Tejedor, and L. Quiroga, “Universal two-time correlations, out-of-time-ordered correlators and Leggett-Garg inequality violation by edge Majorana fermion qubits,” *ArXiv e-prints* (2018), [arXiv:1802.10522](#).
 - [70] T. E. O’Brien, P. Rožek, and A. R. Akhmerov, “Majorana-Based Fermionic Quantum Computation,” *Physical Review Letters* **120**, 220504 (2018).